Electronic Supplementary Information

Chemiresistive thin-film translating biological recognition into electrical signals: an innovative signaling mode for contactless biosensing

Jian Shu,[a] Zhenli Qiu,[a] Qian Zhou,[b,*] and Dianping Tang[a,*]

[a]Key Laboratory for Analytical Science of Food Safety and Biology (MOE & Fujian Province), Department of Chemistry, Fuzhou University, Fuzhou 350116, China; [b]Institute of Environmental and Analytical Science, School of Chemistry and Chemical Engineering, Henan University, Kaifeng 475004, Henan, China.

Corresponding author information:

E-mails: dianping.tang@fzu.edu.cn (D.T.) & zhouqian@henu.edu.cn (Q.Z.)

Fax: +86 591 2286 6135; Tel.: +86 591 2286 6125

Experimental Section

Chemicals and reagents

The DNA oligomers shown in Table S1 were synthesized and HPLC purified by Sangon Biotech Co. (Shanghai, China). Chloroplatinic acid (H_2PtCl_6), potassium tetrachloropalladate (K_2PdCl_4), and nickel chloride ($NiCl_2$) were obtained from Aladdin (Shanghai, China). Carboxyl groups functionalized magnetic beads (MBs, Dynabeads® MyOne™ Carboxylic Acid, 1 μM) were purchased from Thermo Fisher Scientific. N-(3-dimethylaminopropyl)-N′-ethylcarbodiimide hydrochloride (EDC), 2-(N-morpholino) ethanesulfonic acid (MES), sodium borohydride ($NaBH_4$), ammonia borane (AB, NH_3BH_3), N-hydroxysuccinimide (NHS) and sodium citrate were purchased from Sigma-Aldrich. Ultrapure water derived from a Millipore water purification system (Z18 MΩ, Milli-Q, Millipore) was used throughout all experiments. All other reagents were analytically pure and purchased from Sinopharm Chemical Reagent Co., Ltd. (Shanghai, China).

Table S1 The list of the oligonucleotide sequences

Oligonucleotide	Sequence (5'-3')
Capture DNA	5'-NH_2-C_6-AAAAAAAAAA**TATTAACTTTACTCC**-3'
Target DNA	5'-TCAGCGGGGAGGAAG**GGAGTAAAGTTAATA**-3'
Hairpin probe 1(H_1)	5'-Biotin-TEG-CTTCCTCCCCGCTGA*CAAAGTTCAGCGGGG*-3'
Hairpin probe 2(H_2)	5'-TCAGCGGGGAGGAAG*CCCCGCTGAACTTTG*-TEG-Biotin-3'
Single-base mismatch	5'-TCAGCGGGGAGGAAGGGAGTAAAGTT**G**ATA-3'
Two-base mismatch	5'-TCAGCGGGGAGGAAGGGAG**A**AAAGTTAA**C**A-3'
Non-complementary	5'-CGCTAGTCTATAGCCTTGAAAC-3'
Capture aptamer	5′-**TTAACTTATTCGACCATA**TTTTTTTTTT-C_6-NH_2-3′
Trigger aptamer	5′-AGTCTAGGATTCGGCGTGGGTTAATTTTTT**CCCATAGGGAAGTGGGGGA**-3′
Hairpin probe 3 (H_3):	5'-Biotin-TEG-TTAACCCACGCCGAATCCTAGACT*CAAAGTAGTCTAGGATTCGGCGTG* -3'
Hairpin probe 4 (H_4):	5'-AGTCTAGGATTCGGCGTGGGTTAA*CACGCCGAATCCTAGACTACTTTG*-TEG-Biotin-3'

The sequences in bold are recognition sequences for targets and blue sequences are designed for triggering hairpin (H_1 or H_3)

opening; The underlined sequences and italicized sequences within the hairpin probes are the loop and complementary sequences between the first pair of hairpin probes.

Fabrication of chemiresistive thin-film electrode

The palladium nanoparticles-decorated partially reduced graphene oxide (Pd-PRGO) film that coated on the interdigital electrode is obtained by dipping technology and subsequentt hydrazine vapor reducing. The light brown GO is obtained according to the reported method.[S1] K_2PdCl_4 (1 mL, 10 mM) aqueous solution is added into homogeneous GO dispersion (10 mL, 0.5 mg mL^{-1}) and stirred for 0.5 h at room temperature (RT). The mixture is centrifuged and used as precursor solution (10 mL, 0.5 mg mL^{-1}) for dip-coating. Prior to fabricate thin-film electrode, the Au interdigital electrode (2×1 cm) with 37 pole-pairs is orderly cleaned with acetone, alcohol, and water. The electrode is immersed into the precursor solution and lifted vertically from the solution at the speed of 500 nm s^{-1} at RT. Finally, the brown film electrode is reduced to brownish-gray in hydrazine vapor at 40 °C for 1 h.

Preparation of platinum-nickel bimetallic nanoparticles (PtNi NPs)

Citrate-stabilized PtNi NPs are prepared according to the previously reports with a modification.[S2] Briefly, 1.6 mL of H_2PtCl_6 (20 mM) and 0.4 mL of $NiCl_2$ (20 mM) are mixed with 20 mL of sodium citrate (50 mM) aqueous solution. After stirring for 5 min, 3 mL of the freshly prepared $NaBH_4$ (50 mM) solution is quickly added into the above solution and further stirred for 30 min. The PtNi NPs with the average diameter of 4 nm is obtained (1.28 mM, accounted with molar concentration of Pt atom) after removing excess electrolyte by high speed centrifugation.

Preparation of streptavidin conjugated PtNi NPs (PtNi NPs-SA)

The streptavidin conjugated PtNi NPs are prepared according to the previously reported method.[S3] Briefly, streptavidin (50 μL, 0.5 mg mL^{-1}) is added into 0.5 mL of PtNi NPs colloidal dispersion in PBS buffer (pH 6.5, 10 mM) and incubates on a shaker for 20 h (4 °C). Then, BSA (0.1 %, 0.1 mL) solution is added and further incubates for 4 h to block the surface of PtNi NPs. Next, the PtNi NPs-SA complexes is purified by centrifugation to removed unconjugated proteins.

Construction of capture DNA or capture aptamer modified magnetic beads

Capture DNA (cDNA) or capture aptamer (CA) is bound to the magnetic beads (MBs) by a covalent cross-linking reaction between the carboxyl of magnetic beads and amines of cDNA (or CA) (Scheme S1).[S4]

According to the instructions for use, initially, the MBs (50 μL, 1 mg mL^{-1}) are washed twice with equal volume of MES buffer (0.1 M, pH 4.8) and resuspended in 50 μL of MES containing newly prepared 50 mM EDC and 20 mM NHS. After incubation with gentle shaking for 0.5 h, the activated MBs are washed twice with MES. Then, the cDNA (or CA) (0.2 mL, 50 μM) is mixed with the resuspended MBs (0.3 mL) and reacts for 4 hours with gentle shaking. Afterward, the cDNA (or CA) modified MBs is collected by magnetic scaffold and further incubated with Tris (50 mM, pH 7.4) for 15 minutes to quench the non-reacted activated carboxylic acid groups. Repeated wash cDNA (or CA) modified MBs with Tris storage buffer (Tris containing 0.01% Tween-20, pH 7.4) and store it in storage buffer at 4 °C for use.

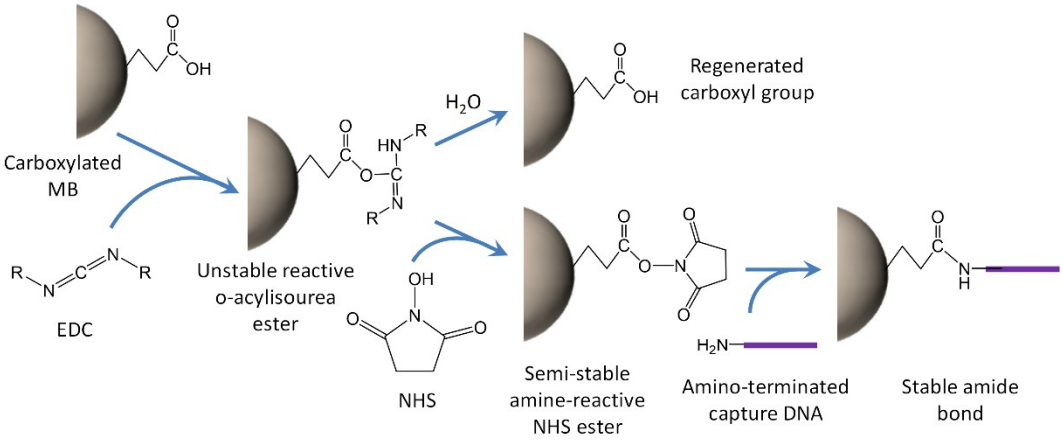

Scheme S1 Crosslinking of carboxylated magnetic beads with amino-terminated capture DNA.

Gel electrophoresis

Prior to use, all the hairpin probes (H1-H4) are initially heated to 95 °C and keep for 2 min, cooling naturally to the room temperature. The DNA samples (7 μL) are mixed with SYBR Green Π solution (2×, 1.5 μL) and loading buffer (6×, 1.5 μL) for 5 min, respectively. A native polyacrylamide gel (12 %) loaded with different samples (6 μL) is run at 110 V for 70 min in TBE buffer solution (1×) and photographed with an autofocus gel imaging system (JS-2012, CHINA)

Catalytic activity evaluation

The experimental design is referenced from previous reported method.[S2b] Briefly, 820 μL of AB (0.5 mg mL^{-1}) is first added into a glass container (capacity of 2 mL) that the top connected with a small hose (Scheme S2). The other end of the hose is connected with a reservoir containing red indicator fluid. The reservoir inserted into a pipette through another small hose. All the connections were sealed with sealant. After PtNi NPs catalyst (130 μL, 128 μM) is quickly injected into the container through the injection pipe,

clamp the pipe with a clip immediately and record the initial value of indicator fluid in the pipette. The volume change of liquid column in the pipette as a result of H_2 generation from the catalytic dehydrogenation of AB with time is recorded continuously. The whole process is operated at 25 °C under ambient atmosphere. The H_2 generation activities in terms of total turnover frequency (TOF) values (mol of H_2·(mol of catalyst·min)$^{-1}$) of PtNi NPs catalyst in hydrolysis of AB is normalized to the molar amount of Pt atom. The catalytic hydrolysis of AB could be briefly expressed as follow:

$$NH_3BH_3 + 2H_2O \xrightarrow{PtNi\ NPs} NH_4^+ + BO_2^- + 3H_2\uparrow$$

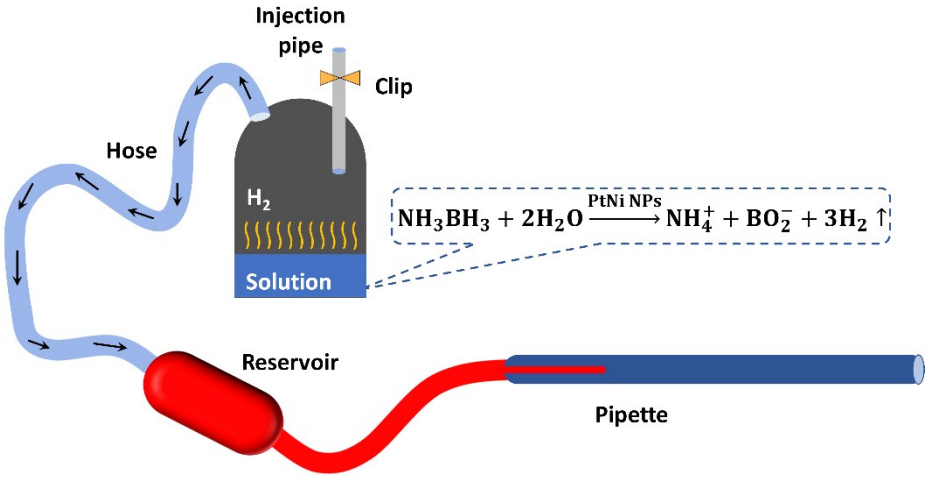

Scheme S2 Schematic drawing of evaluating catalytic activity of PtNi NPs.

Bioassay

All the detection processes are operated at room temperature. Firstly, different concentrations of tDNA or CEA in 20 μL PBS buffer is added to cDNA-MB (20 μL) dispersion and incubated at RT for 35 min. The mixture is separated on a magnetic scaffold for 3 min and washed with PBS solution for 3 times. Then, 20 μL of PBS buffer containing 1.0 μM of various composition (H1 and H2 for DNA detection; H3, H4 and trigger aptamer for CEA detection) is injected and further incubates for 60 min. During this process, the sandwiched reaction and hybridization chain reaction occur simultaneously. Subsequently, separation and wash are performed followed by 50 μL of the PtNP-SA injected. After the mixture further incubates for another 30 min, the resulting MBs are separated and transferred to detection cell to catalyze AB (0.5 mg mL^{-1}) dehydrogenation. At the same time, the current of film electrode in gas phase is continuously recorded under the voltage of 0.2 V by a CHI850D Electrochemical Workstation. Here, the sensor response (R) is defined as $R=(I_a-I_g)/I_a$ in which I_a and I_g represent the steady-state current of the sensor measured in ambient air and in air containing certain concentration of H_2, respectively. The response (or recovery) time

is defined as the period in which the response of a sensor increases to 90 % (or decreases to 10 %) of the max response value toward H_2 with a given concentration

Additional Results and Discussion

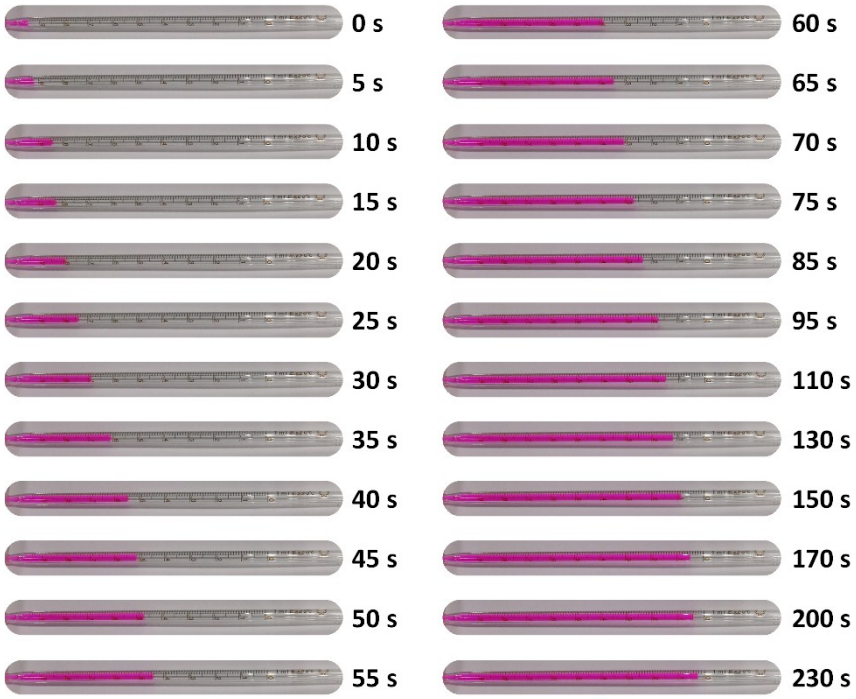

Fig. S2 Photographs of the volume change of liquid column in the pipette as a result of H_2 generation from the catalytic dehydrogenation of AB with time.

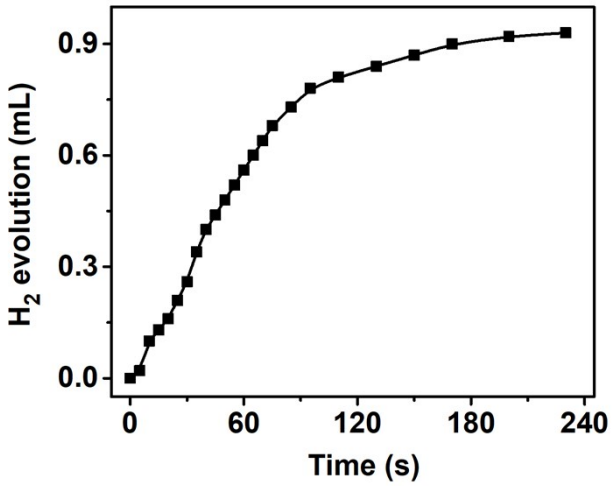

Fig. S3 Plot of time versus volume of H_2 produced from dehydrogenation of AB (820 μL, 0.5 mg mL^{-1}) catalyzed by PtNi NPs (130 μL, 128 μM).

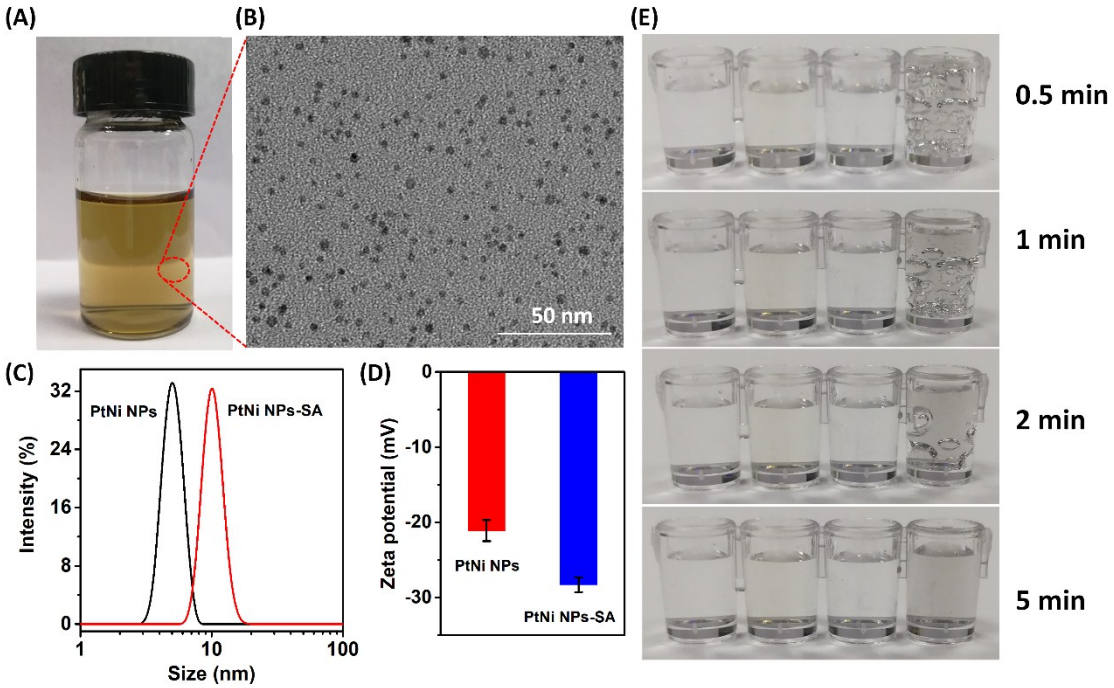

Fig. S4 (A) Photograph and (B) TEM image of PtNi NPs. (C) Zeta potential and (D) hydrodynamic diameter distribution (the error bars represent the standard deviation of three-parallel tests) of PtNi NPs and PtNi NPs-SA. (E) Photographs of characteristic H_2 gas bubbles are observed when PtNi NPs-SA is added to AB solution (from left to right: H_2O, PtNi NPs-SA, AB solution, and AB solution + PtNi NPs-SA).

The synthesized PtNi NPs display excellent dispersibility and uniform size distribution (average grain diameter of 4 nm) (Fig. S4A-B). After conjugating PtNi NPs with streptavidin, the hydrodynamic diameter and zeta potential change from 4 (polydispersity index: 0.042) to 10 nm (polydispersity index: 0.047) and from -21 to -28 mV, respectively (Fig. S4C-D). The AB fizzed up as the result of dramatically generating H_2 when PtNi NPs-SA are added (Fig. S4E). The gas bubbles engendered from the decomposition of AB are released quickly, demonstrating the high catalytic activity remained after conjugation.

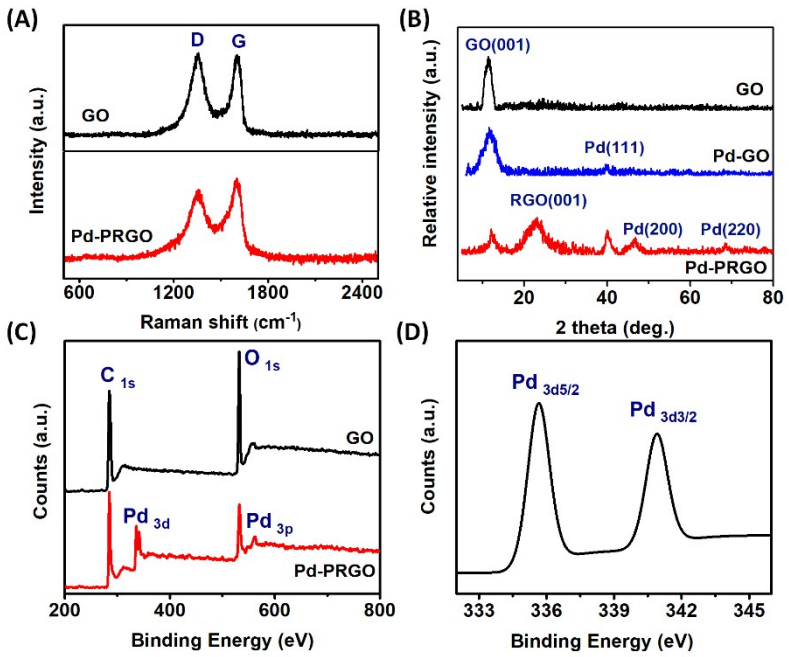

Fig. S5 (A) Raman spectra of GO and Pd-PRGO. (B) XRD patterns of GO (black curve), mixture of GO and K_2PdCl_4 (blue curve), and Pd-PRGO (red curve). (C) XPS survey spectra of GO and Pd-PRGO. (D) High-resolution XPS of Pd 3d.

Raman spectra of the sensing film before and after treated with hydrazine vapor are shown in Fig. S5C. The two bands centered at 1355 cm^{-1} and 1602 cm^{-1} should be ascribed to D band and G band of graphene matrix, respectively. The ratio of peak intensity (I_D/I_G) decreases from 1.01 to 0.87 after treated with hydrazine vapor, which indicates the reduction in some extent of GO and the existence of some structural defects.[S5] The powder X-ray diffraction analysis (XRD) shows the mixture of K_2PdCl_4 and GO exhibits not only diffraction peak of GO (2θ = 10.9 °), but a weak peak that could be ascribed to the PdNPs (2θ = 40.2°).[S6] This result indicates that the $PdCl_4^{2-}$ is reduced to PdNPs with accompanying oxidation of GO in the mixing process.[S7] After treating with hydrazine vapor, both the intensity of typical peak of reduced graphene oxide (RGO, 2θ = 21.5 °) and of PdNPs increased, but the weak peak of GO still exists, which suggest the more PdNPs are formed and the GO is partially reduced by hydrazine vapor. The peak intensity of O_{1s} in XPS spectra of Pd-PRGO significantly decreases by comparing with pristine GO, which directly demonstrates the loss of the oxygen component.[S8] Additionally, the high-resolution XPS spectra of Pd3d clearly showing a binding energy of 335.4 eV, demonstrates the presence of metallic Pd.

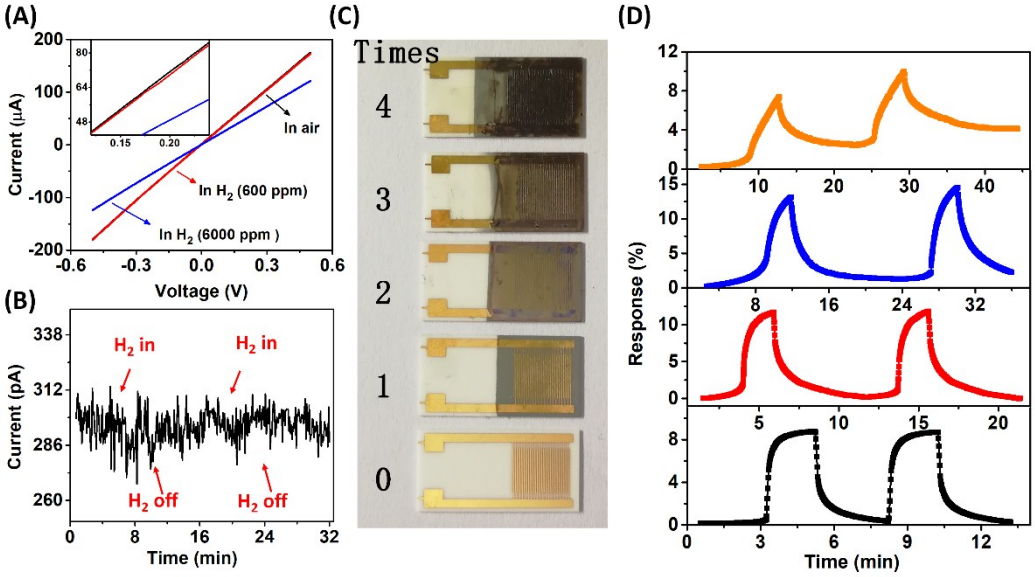

Fig. S6 (A) *I*−*V* characteristic of Pd-PRGO thin film with different H_2 concentrations. (B) Current of bare electrode recorded in air and H_2 atmosphere. (C) Photographs and (D) sensing properties of thin film electrodes with different lifting times.

With the lifting times increase, the thickness and the roughness of sensing film increases obviously. Properly increasing the thickness of film could improve the response. An excessively thick coating not only decreases the sensitivity, but also significantly extends the time for response and recovery.

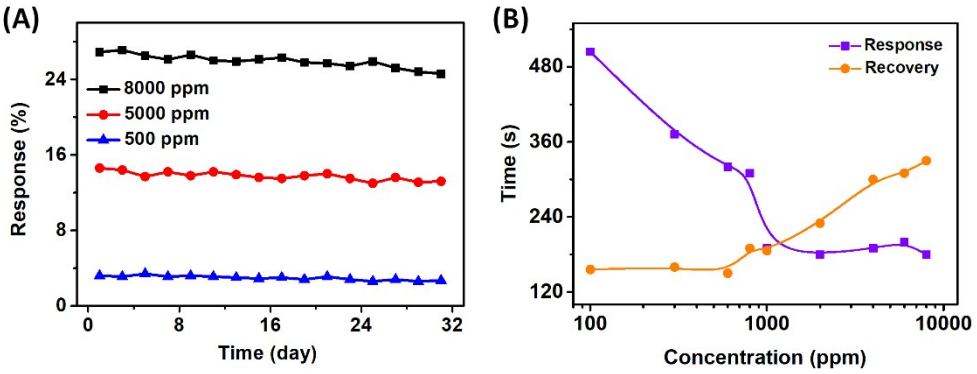

Fig. S7 (A) Long-term stability evaluation. (B) Time for response and recovery of the thin film to H_2 with different concentrations

Different from the gas sensing characteristics in our previous reports,[S9] the opposite change tendency of the time for response and for recovery with the level of H_2 is observed (Fig. S7B). Response is delayed under low concentration H_2 atmosphere because there is not enough available H_2 molecules to rapidly

diffuse to adsorption sites of Pd NPs. At high concentration, lots of dissolved hydrogen in PdH_x need extra time for reacting with the oxygen in air, which prolongs its recovery time.

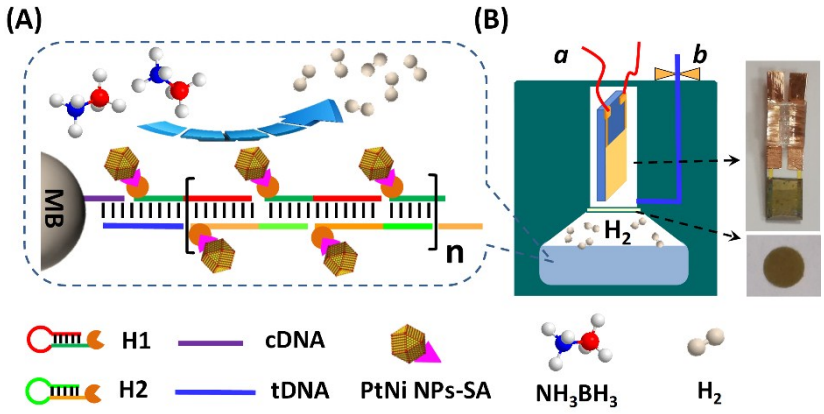

Fig. S8 Schematic illustration of the structure for tDNA detection (A) and the detection device (B) (*a*: current readout; *b*: volume readout).

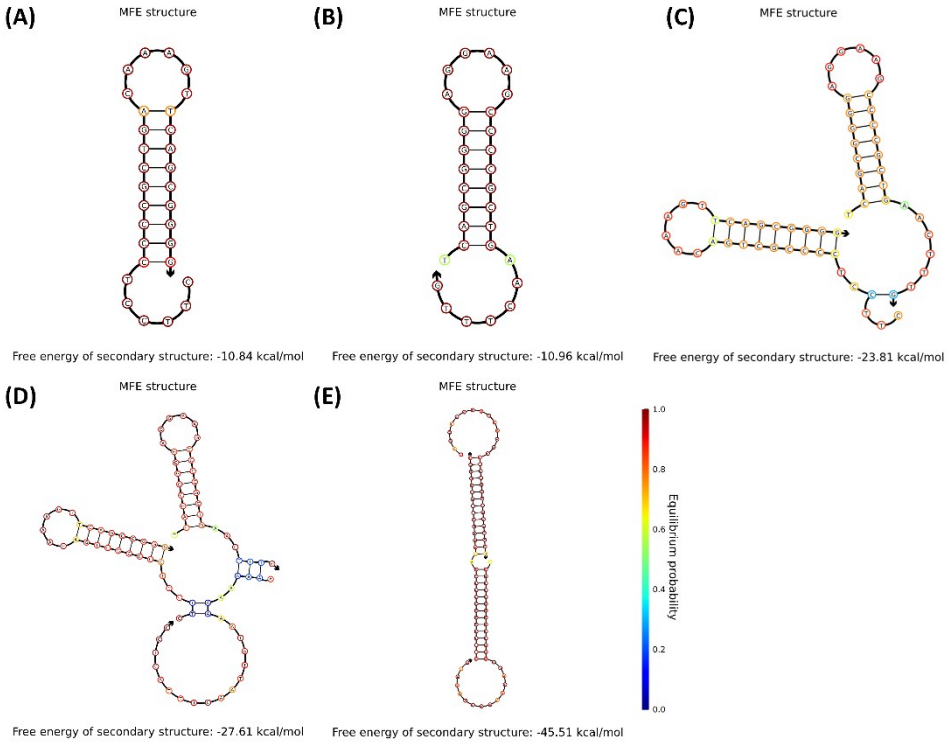

Fig. S9 The NUPACK analysis of optimal conformation and free energy about the DNA sequences for tDNA detection: (A) H1; (B) H2; (C) H1+ H2; (D) H1+ H2+cDNA; (E) H1+ H2+tDNA.

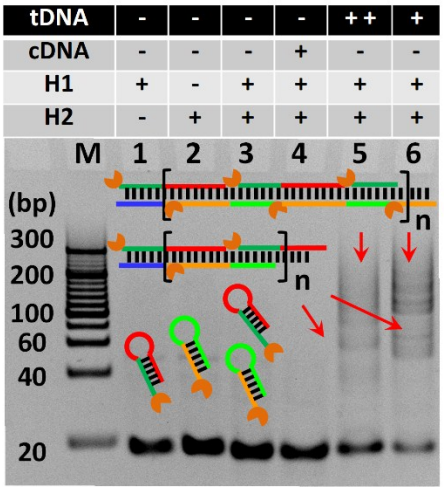

Fig. S10 The PAGE analysis of HCR for DNA detection.

The HCR between two species of biotin-labeled hairpin probes (H1 and H2) is only triggered in the presence of tDNA (lane 5-6). The average length of the produced dsDNA shows a negative correlation with the concentration of tDNA, which is a typical feature of effective HCR.[S10]

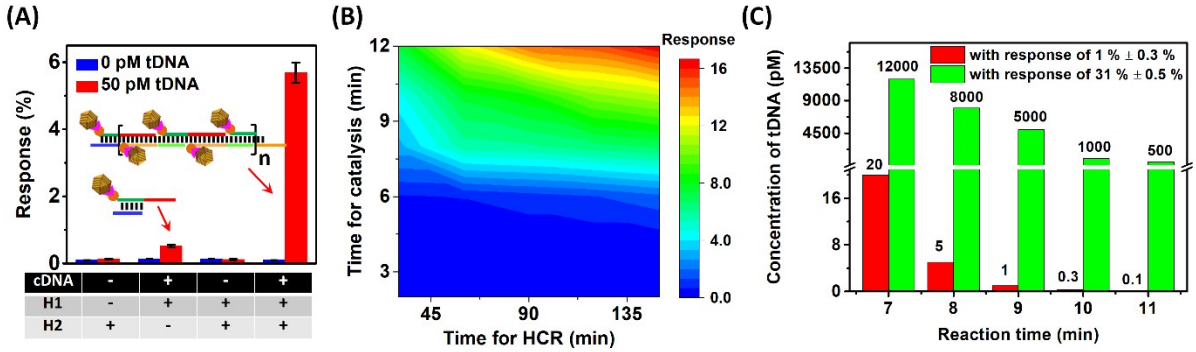

Fig. S11 (A) Response signal recorded under different conditions; (B) The effect of time for HCR and catalysis to response signal (50 pM of tDNA); (C) The detecting range under the different catalyzed reaction time (the concentrations of tDNA resulted a sensor response of 1% and 33% are regarded as the minimum detectable concentration and maximum detectable concentration, respectively.)

Although the time for HCR and hydrogen-producing reaction has impact on the response, the impact of later is more remarkable because the catalytic activity of noble metal catalyst is fairly stable and H_2 is generated continuously (Fig. S11B). Obviously, the detecting range relies heavily on the catalyzed reaction time (Fig. S11C). Weighting from the efficiency, sensitivity and detecting range, appropriately extending the time for catalytic reaction (9 min) and decreasing the time for HCR (60 min) is necessary.

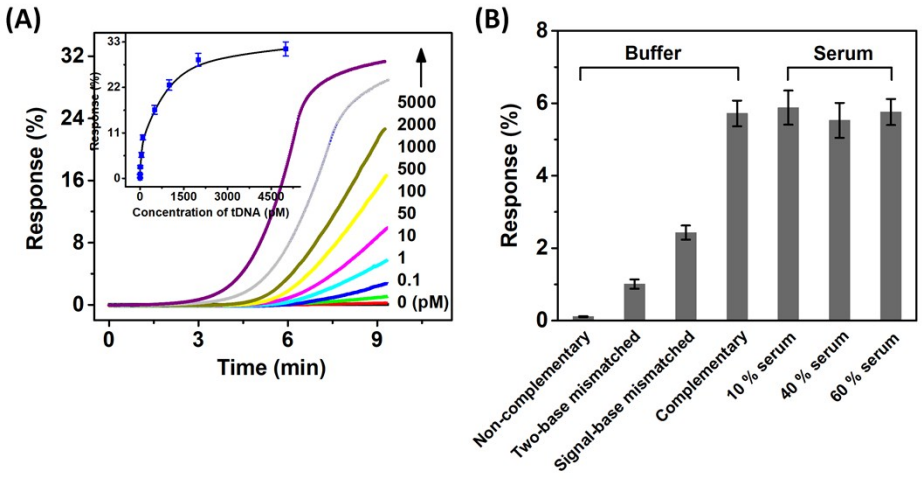

Fig. S12 (A) Response change profiles of GSCB-based platform toward various tDNA concentrations (inset: relations between the response and tDNA concentration at 9 min); (B) DNA specificity tests of the sensing platform.

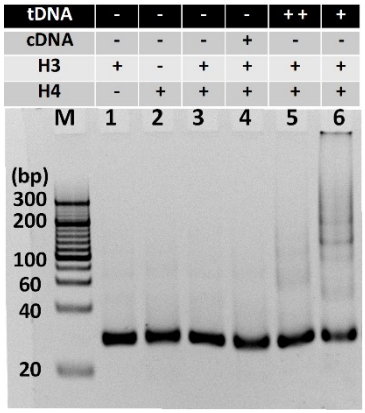

Fig. S13 The PAGE analysis of HCR for CEA detection.

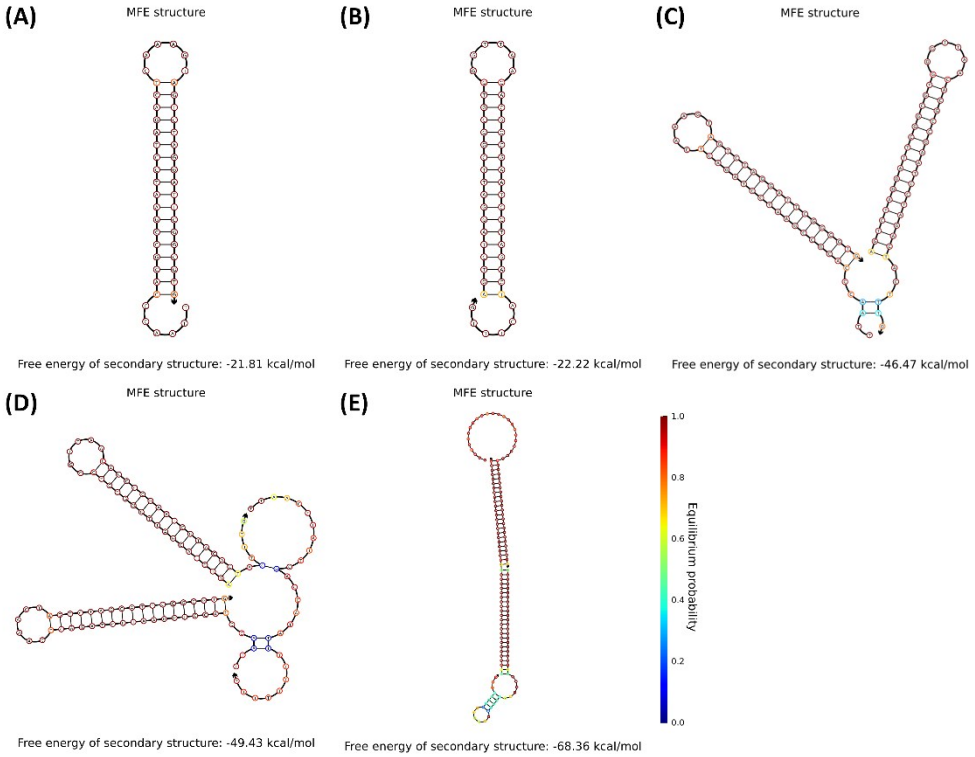

Fig. S14 The NUPACK analysis of optimal conformation and free energy about the DNA sequences for CEA detection: (A) H3; (B) H4; (C) H3+ H4; (D) H3+ H4+capture aptamer; (E) H3+ H4+trigger aptamer

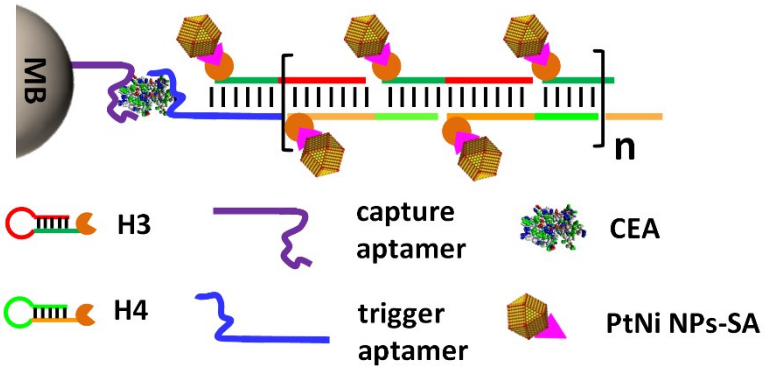

Fig. S15 Schematic illustration of the structure for CEA detection with HCR amplification.

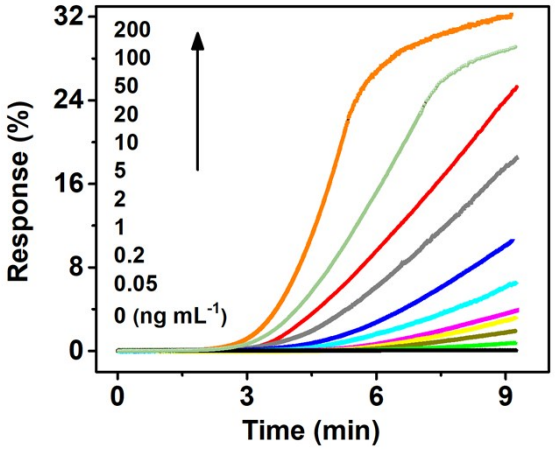

Fig. S16 Response-change profiles of GSCB platform at various CEA concentrations

References

(S1) G. M. Scheuermann, L. Rumi, P. Steurer, W. Bannwarth, R. Mülhaupt, *J. Am. Chem. Soc*. 2009, **131**: 8262.

(S2) (a) S. J. Kwon, A. J. Bard. *J. Am. Chem. Soc.,* 2012, **134**: 10777; (b) S. Wang, D. Zhang, Y. Ma, H. Zhang, J. Gao, Y. Nie, X. Sun, *ACS Appl. Mater. Interfaces,* 2014, **6**, 12429.

(S3) (a) Y. Song, X. Xia, X. Wu, P. Wang, L. Qin, *Angew. Chem. Int. Ed.,* 2014, **53,** 12451; b) Y. Wang, G. Zhu, W. Qi, Y. Li, Y. Song, *Biosens. Bioelectron.,* 2016, **85**, 777.

(S4) C. Y. Wen, L. L. Wu, Z. L. Zhang, Y. L. Liu, S. Z. Wei, J. Hu, *ACS Nano,* 2014, **8**, 941.

(S5) A. Omidvar, B. Jaleh, M. Nasrollahzadeh, *J. Colloid Interface Sci.,* 2017, **496**, 44; (b) J. Shu, Z. Qiu, Q. Wei, J. Zhuang, D. Tang, *Sci. Rep*., 2015, **5**, 15113.

(S6) S. Moussa, A. R. Siamaki, B. F. Gupton, M. S. El-Shall, *ACS Catal*., 2012, **2**, 145.

(S7) X. Chen, G. Wu, J. Chen, X. Chen, Z. Xie, X. Wang, *J. Am. Chem. Soc*., 2011, **133**, 3693.

(S8) S. Wang, L. Zhang, Z. Xia, A. Roy, D. W. Chang, J. Baek, L Dai, *Angew. Chem*., 2012, **124**, 4285.

(S9) (a) J. Shu, Z. Qiu, D. Tang, *Anal. Chem*., 2018, *90*, 9691; (b) J. Shu, Z. Qiu, S. Lv, K. Zhang, D. Tang, *Anal. Chem*., 2017, ***89,*** 11135.

(S10) Z. Ge, M. Lin, P. Wang, H. Pei, J. Yan, J. Shi, Q. Huang, D. He, C. Fan, X. Zuo, *Anal. Chem.,* 2014, **86**, 2124.